AD-A118 158 NAVAL AIR DEVELOPMENT CENTER WARMINSTER PA AIRCRAFT --ETC F/G 11/6
AN EVALUATION OF FRETTING AT SMALL SLIP AMPLITUDES.(U)
JUL 82 P KENNEDY
UNCLASSIFIED NADC-81205-60 NL

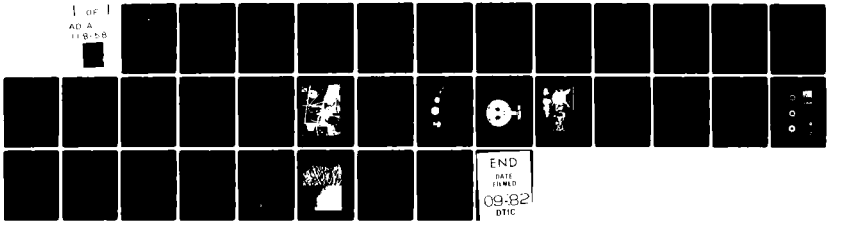

REPORT NO. NADC-81205-60

AN EVALUATION OF FRETTING AT SMALL SLIP AMPLITUDES

Paul Kennedy
Aircraft and Crew Systems Technology Directorate
NAVAL AIR DEVELOPMENT CENTER
Warminster, Pennsylvania 18974

30 July 1982

STATUS REPORT
AIRTASK A-320-320A/001-B/1F61-542-000
WORK UNIT ZM510

APPROVED FOR PUBLIC RELEASE: DISTRIBUTION UNLIMITED

Prepared for
Naval Air Systems Command
Department of the Navy
Washington, DC 20361

NOTICES

REPORT NUMBERING SYSTEM - The numbering of technical project reports issued by the Naval Air Development Center is arranged for specific identification purposes. Each number consists of the Center acronym, the calendar year in which the number was assigned, the sequence number of the report within the specific calendar year, and the official 2-digit correspondence code of the Command Office or the Functional Directorate responsible for the report. For example: Report No. NADC-78015-20 indicates the fifteenth Center report for the year 1978, and prepared by the Systems Directorate. The numerical codes are as follows:

CODE	OFFICE OR DIRECTORATE
00	Commander, Naval Air Development Center
01	Technical Director, Naval Air Development Center
02	Comptroller
10	Directorate Command Projects
20	Systems Directorate
30	Sensors & Avionics Technology Directorate
40	Communication & Navigation Technology Directorate
50	Software Computer Directorate
60	Aircraft & Crew Systems Technology Directorate
70	Planning Assessment Resources
80	Engineering Support Group

PRODUCT ENDORSEMENT - The discussion or instructions concerning commercial products herein do not constitute an endorsement by the Government nor do they convey or imply the license or right to use such products.

APPROVED BY: _____ DATE: 9/28/82

T. J. GALLAGHER
CAPT, MSC, USN

UNCLASSIFIED

SECURITY CLASSIFICATION OF THIS PAGE (When Data Entered)

REPORT DOCUMENTATION PAGE		READ INSTRUCTIONS BEFORE COMPLETING FORM
1. REPORT NUMBER NADC-81205-60	2. GOVT ACCESSION NO. AD-A118 158	3. RECIPIENT'S CATALOG NUMBER
4. TITLE (and Subtitle) AN EVALUATION OF FRETTING AT SMALL SLIP AMPLITUDES		5. TYPE OF REPORT & PERIOD COVERED Status Report 6. PERFORMING ORG. REPORT NUMBER
7. AUTHOR(s) Paul Kennedy		8. CONTRACT OR GRANT NUMBER(s)
9. PERFORMING ORGANIZATION NAME AND ADDRESS Naval Air Development Center Aircraft and Crew Systems Technology Directorate Warminster, Pennsylvania 18974		10. PROGRAM ELEMENT, PROJECT, TASK AREA & WORK UNIT NUMBERS AIRTASK A-320-320A/001-B/ 1F61-542-000, Work Unit ZM510
11. CONTROLLING OFFICE NAME AND ADDRESS Naval Air Systems Command Department of the Navy Washington, DC 20361		12. REPORT DATE 30 Jul 1982 13. NUMBER OF PAGES 30
14. MONITORING AGENCY NAME & ADDRESS(if different from Controlling Office)		15. SECURITY CLASS. (of this report) UNCLASSIFIED 15a. DECLASSIFICATION/DOWNGRADING SCHEDULE
16. DISTRIBUTION STATEMENT (of this Report) Approved for Public Release; distribution unlimited.		
17. DISTRIBUTION STATEMENT (of the abstract entered in Block 20, if different from Report)		
18. SUPPLEMENTARY NOTES		
19. KEY WORDS (Continue on reverse side if necessary and identify by block number) Fretting, Wear, Tests, Friction, Metal, Carbon Steel, Microslip		
20. ABSTRACT (Continue on reverse side if necessary and identify by block number) Fretting wear and resulting surface damage produced by the twisting motion of a flat steel specimen against a fixed 12.7 mm steel ball, has been investigated in the limited microslip region ranging from 0.05 to 5.0 μm. The construction of the test rig and the type of fretting wear associated with this particular specimen configuration and motion are discussed. This discussion covers data obtained either with SAE 52100 steel or Hastelloy B ball specimens in combination with SAE 1018 steel flat specimens.		

DD FORM 1 JAN 73 1473 EDITION OF 1 NOV 65 IS OBSOLETE
S/N 0102-014-6601

UNCLASSIFIED

SECURITY CLASSIFICATION OF THIS PAGE (When Data Entered)

These data were found to conform to elastic theory, developed for this type of contact. It was found that the first indication of metal oxidation associated with the onset of fretting occurred at a slip amplitude of about 0.075 μm. Severe damage was noted at 2.5 μm.

TABLE OF CONTENTS

LIST OF TABLES

LIST OF FIGURES

LIST OF FIGURES

BACKGROUND

Fretting, particularly in its relationship to reduced fatigue strength and increased wear, constitutes a serious problem in both fixed and rotary winged aircraft. The list of aircraft components subjected to fretting damage is lengthy and includes parts such as splines, cables, bearings, hinges, seals and actuating devices. The list of proposed solutions for fretting problems is also extensive and involves techniques such as the use of special surface finishes, shims, adhesives, lubricants, coatings and if necessary, design changes to control fretting. Finding the correct solution to a given fretting problem usually relies fairly heavily on the "trial and error" approach. Furthermore, it has been found that a solution for one problem is not always successful when applied to another problem. As a result, tests must be conducted in the actual application; this is an expensive and time consuming process. This work was undertaken in order to find a scientific approach to the selection of solutions for fretting problems. Previous experimental studies of fretting have considered the effect of a variety of variables (1), (2), (3), (4) with major empnasis on stress, number of cycles, amplitude, frequency, and atmosphere. To make such information useful in solving the component problems in aircraft, some parameter must be selected which can be predicted in design and correlates well with the severity of the fretting. A review of these studies indicated that slip amplitude may be such a parameter.

A number of investigators have shown that damage will not occur if the slip is limited to the elastic region (5), (6). Others (7), (8), (9) have shown that the wear rate increases significantly when the slip amplitude is greater than about 70 μm. Thus, it is clear that both surface damage and wear increase in some manner with increase in slip amplitude. Complete data for a given material combination would yield plots of wear rate and surface damage (measured as roughness) as a function of slip amplitude.

To use this data in aircraft design or failure investigation, it would first be necessary to measure or predict the slip amplitude in the application. With this information, the amount of wear or damage at that amplitude can be determined by referring to the graphs for the specific materials in use. If this level of wear or damage is unacceptable, the designer can either change the design to lower the slip amplitude, or select another material combination with an acceptable damage level.

One premise (10) that would explain the effect of slip amplitude on fretting is that fretting is dependent on the simultaneous or subsequential occurrence of two or more different wear processes such as adhesion, oxidation, fatigue and abrasion. The possibility of different wear mechanisms operating under different conditions could help to explain why a certain fretting countermeasure might be effective under one set of conditions but detrimental under a different set of conditions (11), (12). This would also explain the relationship of wear rate to slip amplitude. For example, several investigators who had studied the effect of slip

amplitude on fretting wear in the 10 to 1000 μm range, had reported the existence of characteristic slip amplitudes, usually somewhere between 30 to 70 μm, at which the fretting wear rate may increase by several orders of magnitude (7), (8), (13). Below this critical amplitude, wear rates were found to be small and normally difficult to measure.

This study is initially concerned with the 0 to 10 μm range where surface damage rather than wear occurs. This change is important since it is also associated with the initiation of the fatigue process. Another area of interest is the mechanistic differences in the fretting process at small and large slip amplitudes. If significant differences were found, then it would follow that different material and lubricant solutions might apply at different slip amplitudes or that an understanding of this effect could possibly lead to the development of lubricant solutions dependent on the amplitude of microslip.

In addition to being a sensitive indicator of changes in the fretting wear process, slip amplitudes can also serve as an aid in the understanding of the fretting process.

EXPERIMENTAL

TEST APPARATUS

A test apparatus previously used in pivot fretting studies (10) was adapted for this investigation. A photograph and schematic of the test rig are shown in Figures 1 and 2. This test rig provides for mounting of a ball against a flat test specimen. For the sake of clarity, certain components such as labyrinth seals and a special holder for the flat specimen were omitted from this sketch. These components, along with a typical ball and flat specimen are shown in Figure 3. In this test rig, the ball is attached to the metal shaft in a special labyrinth seal arrangement and the flat is attached to the gas bearing using the holder shown in Figure 3.

The metal shaft shown in Figure 2 is held in place by means of two thin metal diaphragms. This shaft is rigidly attached to a metal diaphragm immediately below the bellow type load cell. The lower metal diaphragm serves mostly as a guide for the shaft and also to prevent lateral movement. Application of air pressure to the load cell results in a downward flexing of the upper metal diaphragm which in turn produces a downward movement of the ball. Under load conditions, the ball is held rigidly stationary against the flat specimen.

The flat specimen in Figure 2 is rigidly attached to the gas bearing. The gas bearing is essentially a metal hemisphere as shown in Figure 4. A top view of the gas bearing with the flat specimen attached is shown in Figure 3. This gas bearing fits into a spherical seat, Figure 5, in the base plate that conforms to the outer geometry of the gas bearing. In operation, the gas bearing floats on a thin film of air that separates the bearing from its spherical seat. This floating or lifting of the gas

bearing is achieved by forcing air through small orifices located on the surface of the spherical seat. Application of air pressure to the base of this rig results in an upward movement of the flat specimen. Loading of the ball against the flat specimen is achieved through balancing the air pressure applied to the load cell against the air pressure supplied to the gas bearing so that the amount of gas bearing lift will remain at some preselected value.

Controlled movement of the flat specimen was achieved through the use of two electromagnetic drive units attached to the gas bearing lever arm. These components and linkages are shown in Figure 5 and schematically in Figure 6. The drive units consist of two low internal mass 75 Watt audio speakers modified by fastening an aluminum cone and push rod assembly on to the surface of the speaker cone. This assembly transmits the vibratory motions of the speaker cones to the lever arm of the gas bearing. The amplitude, frequency and phase relationship of the motion of the push rods are controlled through the use of an oscillator and amplifier in the electrical circuit used to power the drive units. These parameters were monitored by capacitance probes positioned at the points of attachment of the push rods to the lever arm of the gas bearing. The point of contact of the ball with the flat specimen serves as a pivot point for all applied motion. In this study, the drive units were operated in-phase in order to achieve a twisting motion. This oscillatory rotational movement of the flat specimen is indicated in Figure 6 by the curved arrows. Although the out-of-phase operation of the drive units was not investigated, this mode of operation would produce a rocking of the flat specimen about the ball/flat pivot point.

WEAR SCAR ANALYSIS

An analysis of a typical wear scar is presented in Figure 7. This analysis considers a ball resting on a rigid plate. This ball is subjected to a normal load, ω, and a tangential force or shear force, F, acting normal to the load and in the plane of the flat plate. The area of contact for a ball resting on a flat plate is a circle having a radius defined by the Hertz equation (10, 15)

$$a = 0.881 \sqrt[3]{\frac{PD}{E}} \qquad (1)$$

where: a = radius of contact area
P = applied load
D = diameter of the ball
E = elastic modulus

This equation indicates that the radius of the contact area is dependent only on the applied load if the material and the diameter of the ball are held constant. The diameter of this contact area is indicated by the outer set of dash lines in Figure 7. A value for the maximum pressure or maximum normal stress (T_N, max) can also be calculated from the Hertz equations (10, 15). These equations indicate that the normal stress

T_N, would be at a maximum at the pivot point and would approach zero at the contact edge. A graphical representation of a possible normal stress distribution along the contact area is shown. The shear stress, T_S, also graphically represented, would be zero in the center at the pivot point and would approach a maximum at the edge.

A sketch of a typical wear scar is shown at the bottom of Figure 7. No wear damage can occur in the central unshaded region. This region is normally defined as a locked region. Microslip and surface damage is limited to the outer shaded region, which can be called the slipped region. This type of wear pattern is a result of the distribution of shear stress relative to normal stress. In order to have slippage or relative motion of the ball against the flat, a necessary condition would be that the ratio of the two stresses $T_S/T_N > f_s$ (where f_s is the static coefficient of friction for the material pair). At the center or pivot point, the ratio of shear to normal stress would be at a minimum. Proceeding outward from the center along radius r, this ratio would be expected to increase until at some point, this ratio would equal the static coefficient of friction for the pair. This point would define the boundary between the locked and slipped regions. Prior to this point or when $T_S/T_N < f_s$, the two surfaces would be locked together and would only be able to undergo elastic deformations. Beyond this point where $T_S/T_N > f_s$, microslip will occur. If a load is applied to the contact area and a torque is also applied, slip will first occur at the outer region since the shear stress is high and the pressure is extremely small. Thus, slip must result from an applied twisting moment no matter how small. Slip would start at the outer edge of the contact and would progress radially inward as the amplitude is increased. At some point where the input torque $F \geq f_s\omega$, slip will occur over the entire region of contact.

CALCULATION OF SLIP AMPLITUDE

In testing, a rigidly held ball is loaded against a flat specimen and fretting damage is produced by the twisting of the flat specimen about the ball/flat pivot point. Figure 6 illustrates the mechanics required to generate this type of motion. In this Figure, the dash lines indicate the relative motion of the lever arm for in-phase operation of the drive units and the large double headed arrows represent the magnitude of the input amplitude. It can be seen from Figure 6 that the displacement of any point on the surface of the flat specimen can be readily calculated using the method of similar triangles. For example, the displacement of a point on the edge of the ball/flat contact area can be determined by multiplying the input amplitude by the ratio of the radius of the contact area to the length of the lever arm. This latter value is approximately 0.02. Since input amplitudes for this type of drive unit range from 2.0 to 150 μm, typical displacements at the edge of the contact area range from 0.04 to 3 μm.

Because of the extremely small magnitudes of the displacements that are being studied, it is important to differentiate between displacement and microslip. Figure 8 shows the relationship of microslip to displacement in the ball/flat contact area. At the edge of the locked region, geometry indicates that a measurable displacement about 0.02 times the

input amplitude will occur, however, theory indicates that this total displacement will be taken up elastically so that the actual microslip will be zero. Although elastic deformation effects are extremely important at the edge of the locked region, this effect is relatively unimportant at the outer edge of the slipped region. Since the contact pressure is zero at the outer edge of the slipped region, elastic deformation will not occur and the slip amplitude would be equal to the measured displacement. In this study, slip amplitudes were calculated at the Hertz radius.

MATERIALS AND OPERATING PROCEDURES

The flat specimens used in this study were machined from SAE 1018 steel rod stock. Specimens were received with an 0.2 μm ground surface finish. Some of these specimens were later hand polished to a mirror finish using 0.3 and 0.05 μm aluminum polishing wheels. Testing was done on both types of surface finishes. Ball specimens were made from either SAE 52100 steel or Hastelloy B. The SAE 52100 steel specimens were standard 12.7 mm grade 25 chrome balls. Prior to use, specimens were cleaned by washing in Stoddard solvent and rinsing in petroleum ether.

The arrangements of the ball and flat specimens in the test rig is shown in Figure 2. Prior to the attachment of air lines, the clearance between the two specimens is of the order of 0.8 mm. Since the gas bearing is usually operated at a lift of 0.025 mm, loading of the ball against the flat is achieved through increased pressure in the load cell. After balancing the air pressure supplied to the base plate against that supplied to the load cell, a twisting type motion is imparted to the flat specimen by means of the electromagnetic drive units. In testing, the ball is stationary and motion is limited to the flat specimen. The amplitude of microslip is adjusted by using the oscillator and amplifier attached to the electromagnetic drive units. Testing was normally done for three hours. After testing, specimens were microscopically examined and some of these specimens were later subjected to surface profile measurements and microprobe analysis.

R E S U L T S A N D D I S C U S S I O N

SAE 52100/SAE 1018 STEEL COMBINATION

Typical wear scars, obtained at various fretting amplitudes, are shown in Figure 9. In this part of the investigation, the test specimen configuration consisted of a 12.7 mm diameter SAE 52100 ball against a highly polished 1018 flat specimen. Fretting experiments were run at 9 kg load and 210 Hz for three hours. The photomicrographs in Figure 9 depict wear scars on the surface of the flat specimens. The corresponding wear scars formed on the balls were identical and are not shown. The photomicrographs in Figure 9 were taken at 100X magnification since these wear scars are small and typically had diameters ranging from 0.3 to 0.5 mm. Average microslip amplitudes are reported above each wear scar.

Visual inspection of the photomicrographs in Figure 9 indicates that a definite, although a minimal amount of fretting damage can occur at

slip amplitudes as low as 0.1 μm. The wear scar diameter under these conditions was the same as that predicted using equation (1). Two tests, made on a polished and an unpolished specimen at an amplitude of 0.05 μm, did not suggest any trace of surface damage. Photographs of the flats used in these latter tests are not included in Figure 9. Surface damage appears to increase dramatically with amplitude in this series. An estimate of 0.075 μm for the minimum amount of microslip necessary to produce surface damage would seem reasonable.

Additional testing, basically under identical conditions, was done on a series of unpolished specimens in order to determine if fretting damage was significantly affected by surface finish. Wear scars on unpolished specimens were found to be for all practical purposes identical to wear scars formed on polished specimens. No surface finish effect was found. Visual inspection of the photomicrographs suggested an exponential type of wear growth with regard to slip amplitude. In order to graphically investigate the possibility, data from both polished and unpolished specimens were combined for use in plotting Figures 10 and 11. The effect of microslip on the outer diameter of the wear scar is shown in Figure 10. Although this data was collected under conditions of constant load, there is a significant increase in the outside diameter of the wear scar with increasing slip amplitude. This may represent surface damage and wear. However, theoretical explanations are possible. Another parameter investigated was the width or the thickness of the slipped region. This width would be equal to the difference in length of the radius of the wear scar less the radius of the locked region. This data is shown in Figure 11. The effect of a small change in amplitude on the width of this area or the amount of surface damage was found to be very pronounced. This relationship is linear in the region ranging from 0.5 to 2.5 μm.

A peculiarity in the fretting wear process was noted at a microslip value of approximately 2.5 μm. In the normal operation of this test rig in the 0 to 2.5 μm region, the power requirements for the electromagnetic drive units were found to be directly proportional to slip amplitude. Also, the power requirement needed to maintain a given slip amplitude did not noticably change during the three hour test period. For amplitudes greater than 2.5 μm, it was found that the power supplied to the electromagnetic drive units needed to be constantly increased throughout the test period in order to maintain the selected slip amplitude. This type of behavior is suggestive of a severe adhesive type wear process and may represent the transition from fatigue wear to adhesive wear.

Visual inspection of the photomicrographs in Figure 9 indicates that the diameter of locked region decreases with increasing slip amplitude. One qualitative explanation for this trend in the data might be based on the previously discussed microslip model which suggests that an increase in shear stress would cause a corresponding decrease in the diameter of the locked region so as to maintain a constant value for the coefficient of friction at the edge of the locked region. The possibility that small amplitude slip, such as would be found near the edge of the locked region, might not produce surface damage, should also be

considered. If this were true, then the occurrence of surface damage on the flat specimen might require a certain minimum slip amplitude and this factor may be primarily responsible for determining the diameter of the locked region. Both explanations would be consistent with each other if it is proposed that a certain region exists outside of the true locked region in which slip can occur without producing any surface damage. This type of wear scar model is shown in Figure 12. This latter possibility was investigated by plotting the amount of displacement or elastic deformation occuring at the outer edge of the locked region as a function of input amplitude. These data, shown in Figure 13, indicate that the amount of displacement at the edge of the locked region increases with increasing input amplitude, but for higher values of input amplitude, the displacement was approximately 1 μm. These data are difficult to interpret since it is not known if the apparent locked region is equal to the true or theoretical locked region.

A quantitative model, capable of predicting the radius of the locked region and the radius of the slipped region as a function of input amplitude, is needed for the correct interpretation of these data. Deresiewicz (14) has developed such a model for two contacting elastic spheres acted upon by a small oscillating torsional couple. In this treatment, the ball on flat geometry translates to a sphere in contact with another sphere of infinite radius. In Deresiewicz's analysis, the ratio of the locked region radius to the Hertz or load radius, c/a, is expressed as a function of the input amplitude, β in equations (2) and (3),

$$c/a = \sqrt[2]{K^2 + 1} \qquad (2)$$

$$\frac{\mu a^2 \beta}{f N} = \frac{3}{16} K^2 \left(1 + \frac{3}{8} K^2 + \frac{15}{64} K^4 + \ldots\ldots \right) \qquad (3)$$

where c = radius of the locked region
a = Hertz or load radius
β = input amplitude in radians
μ = shear modulus
f = coefficient of friction
N = applied load

Using the above equations, theoretical values for the radius of the locked region as a function of input amplitude were calculated. For these calculations, the shear modulus was taken as 10^6, the frictional coefficient was a value of 0.8, the load was 9 kg and the initial load radius was taken as 0.152 mm. The calculated radius of the locked region is compared to the experimentally measured radius of the locked region at different input amplitudes in Table I and these data are graphically represented in Figure 14. It can be seen that this theoretical model correctly predicts that increasing the input amplitude will result in a reduction in the radius of the locked region; however, predicted radii are generally smaller than measured radii. Possible causes for the differences between experimental and calculated data may be surface damage and variances in the coefficient of friction.

HASTELLOY "B" SAE 1018 STEEL COMBINATION

The SAE 52100/1018 steel combination was initially studied since it is a relatively common material combination and because it had been implicated in a Navy related fretting problem. Further studies were carried out using Hastelloy B balls and SAE 1018 steel flats. A typical photomicrograph of a wear scar with an expanded view of the wear track is shown in Figure 15. In this part of the study, photomicrographs were obtained using a scanning electron microscope rather than the previously used optical microscope. The wear scar in Figure 15 was formed on a SAE 1018 steel flat specimen using a Hastelloy B ball. This latter material is a Ni alloy containing a high concentration of Mo. As a result of the significant difference in the metallurgy, flat specimens were subjected to microprobe analysis in order to determine if metal transfer processes had occurred. The results of this study indicated the presence of Fe, Ni and Mo in the slipped region on the flat but no Ni or Mo was detected in the locked region or outside this contact area. The only element found in these latter areas was Fe. This type of data helps to define the actual wear processes that occur under fretting conditions. In this case, actual metal transfer from the ball to the flat did occur.

A knowledge of the morphology of the wear scar is important in order to validate that the test rig is operating properly and also to gain an insight into the type of damage occurring in the slipped region. Traces of the surface profiles for several different wear scars are shown in Figure 16. These traces illustrate the type of damage that was found on the SAE 1018 flat specimens. Data do not suggest any permanent deformation of the flat specimens as a result of loading the Hastelloy B ball against the SAE 1018 steel flat. In these traces, the elevation of the locked region appears to be at the same height as the surface of the flat outside the damaged region. Any waviness in the locked region might possibly be attributed to surface deformation during polishing. This absence of surface deformation is important, since if it had occurred, it would have required a modification of the assumptions concerning the distribution of normal stress in the contact area.

Surface profiles are presented as a function of slip amplitudes in Figure 16. All tests were run for three hours except for one test of an hour duration at 0.53 μm. This later test was included since it shows some evidence of disgorgement of metal from the flat specimen itself. As an approach to monitoring fretting damage, wear volumes were determined from these traces by first determining an average cross sectional area and then multiplying this value by the length of the average circumference of the slipped region. These data are shown in Figure 17. The calculated wear volumes were found to be extremely small, but the data did indicate an exponential relationship between wear volume and slip amplitude. It is apparent that surface damage began in the 0.08 to 0.53 μm range. A value of 0.075 was found for the SAE 52100/SAE 1018 combination in the previous section.

C O N C L U S I O N S

The data contained herein are preliminary. However, they show that

this testing device can generate highly reproducible wear scars having characteristics highly dependent on slip amplitudes. Important parameters related to the fretting process, such as a characteristic slip amplitude associated with the first evidence of mild oxidative fretting, and what appears to be an apparent characteristic slip amplitude associated with the onset of severe adhesive wear, have been identified and determined from wear data. In the first case, this characteristic slip amplitude can be easily determined through visual inspection of wear scars. For example, in the case of the SAE 52100/SAE 1018 steel combination, the first indication of red oxidative wear would be expected at around 0.075 μm. A second limiting parameter of slip amplitude, which is probably more associated with specimen configuration than the fretting process, was found at 2.5 μm. Below 2.5 μm, the frictional characteristics of the metal pair remained essentially constant throughout the test. Above this value, the frictional characteristics tended to increase rapidly.

REFERENCES

1. Waterhouse, R. B., "Fretting Corrosion", Pergamon Press, New York 1972

2. Ohmae, N. and Tzkizow, T., Wear, Vol. 27, 1975, p. 281

3. Gross, G. and Hoeppner, D., Wear, Vol. 27, 1974, p. 153

4. Campbell, W., "Fretting", Chapter 7, Boundary Lubrication, An Appraisal of World Literature, ASME 1969

5. Kan, H., Ashida, M., Terauchi, Y. and Yasunaga, T., Journal of JSLE Vol. 2, 1981, p. 5

6. Johnson, K. L., Proc. Roy. Soc. A, Vol. 231, 1955, p. 531

7. Hurricks, P. L., Wear, Vol. 15 (6) 1970, p. 389

8. Feng, I. M. and Rightmire, B. C., Proceedings Inst. Mech. Eng., Vol. 170, 1956, p. 1055

9. Halliday, J. S., and Hirst, W., Proc. Roy. Soc. (London), Vol. 236, 1956, p. 441

10. Peterson, M. B., Geren, B. F., Arwas, E. B., Gray, S., Murray, S. F., Lund, J. W. and Ling, F. F., Mechanical Technology Incorporated, NASA CR 72609 (MTI TR-32), 1969

11. Begellinger, A. and DeGee, A. W. J., AGARD Conference Proceedings No. 161, National Technical Information Service, Springfield, Virginia, 1974

12. Peterson, M. B., and Gabel, M. B., AGARD Conference Proceedings No. 161, National Technical Information Service, Springfield, Virginia, 1974

13. Waterhouse, R. B., "Fretting Wear", Proceedings of the 1981 International Wear Conference, San Francisco, California, April 1981, ASME, p. 17-22

14. Deresiewicz, H., Journal of Applied Mechanics, Trans. ASME, Vol. 76, 1954, p. 52-56

15. Winer, W. O. and Chang, H. S., "The Wear Control Handbook", ASME, New York, 1980, p. 81

TABLE 1. Comparison of the Theoretical Versus Measured Radii of the Locked Region as a Function of Amplitude

Relative[1] Amplitude (μm)	Average Slip Amplitude (μm)	Theoretical Radius of the Locked Region (mm)	Measure Radius of the Locked Region (mm)	Percent Relative Error
0	0	0.152	0.159	4.6
5.1	0.11	0.150	0.159	6.0
12.7	0.26	0.145	0.162	11.7
25.4	0.53	0.137	0.157	14.6
50.8	1.06	0.117	0.142	21.4
76.2	1.59	0.104	0.110	5.8
101.3	2.12	0.084	0.086	2.5
114.3	2.38	0.081	0.072	-11.1
152.4	3.18	0.066	0.082	24.2

1. Amplitude Measured at the Capacitance Probe

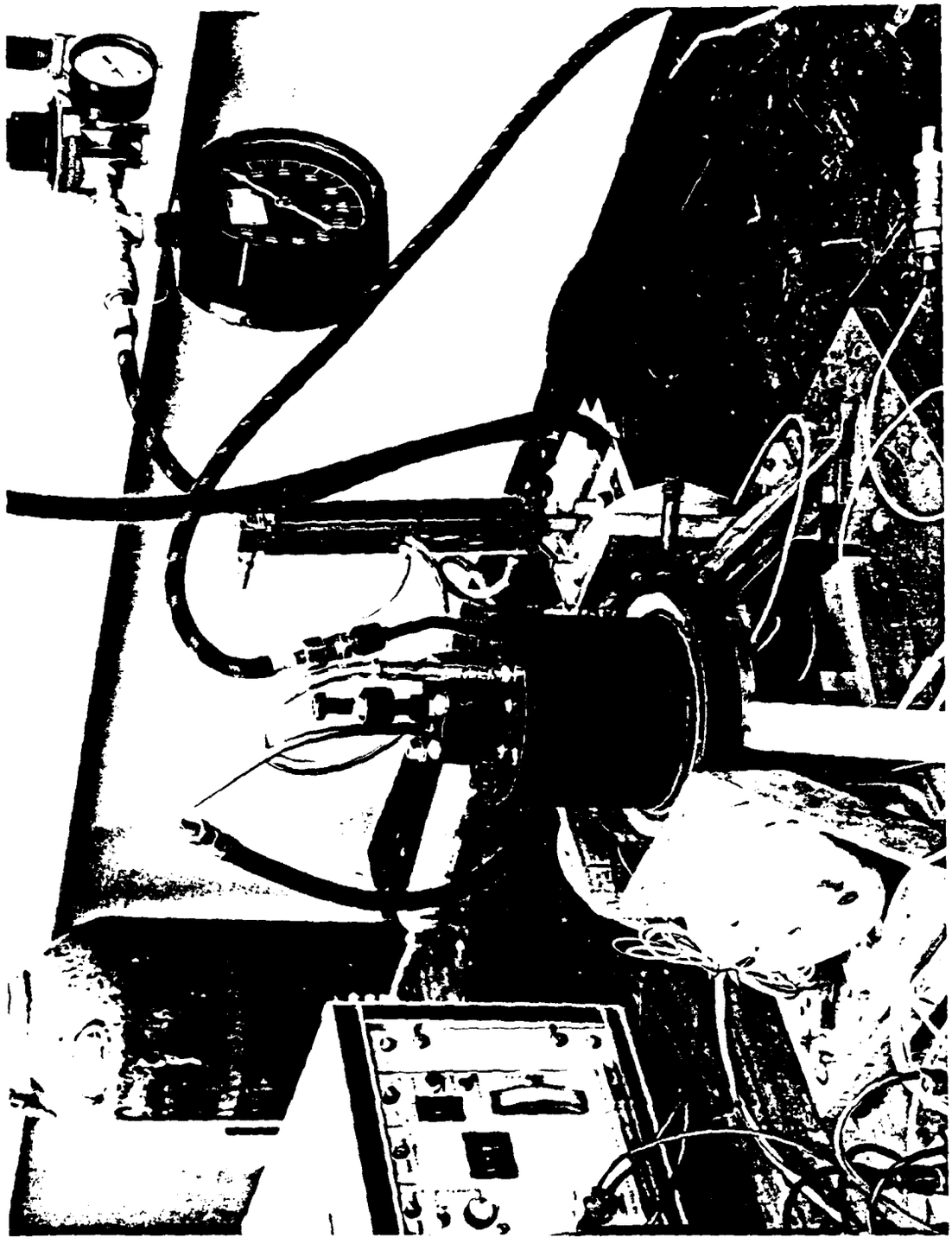

FIGURE 1. PHOTOGRAPH OF FRETTING TEST RIG

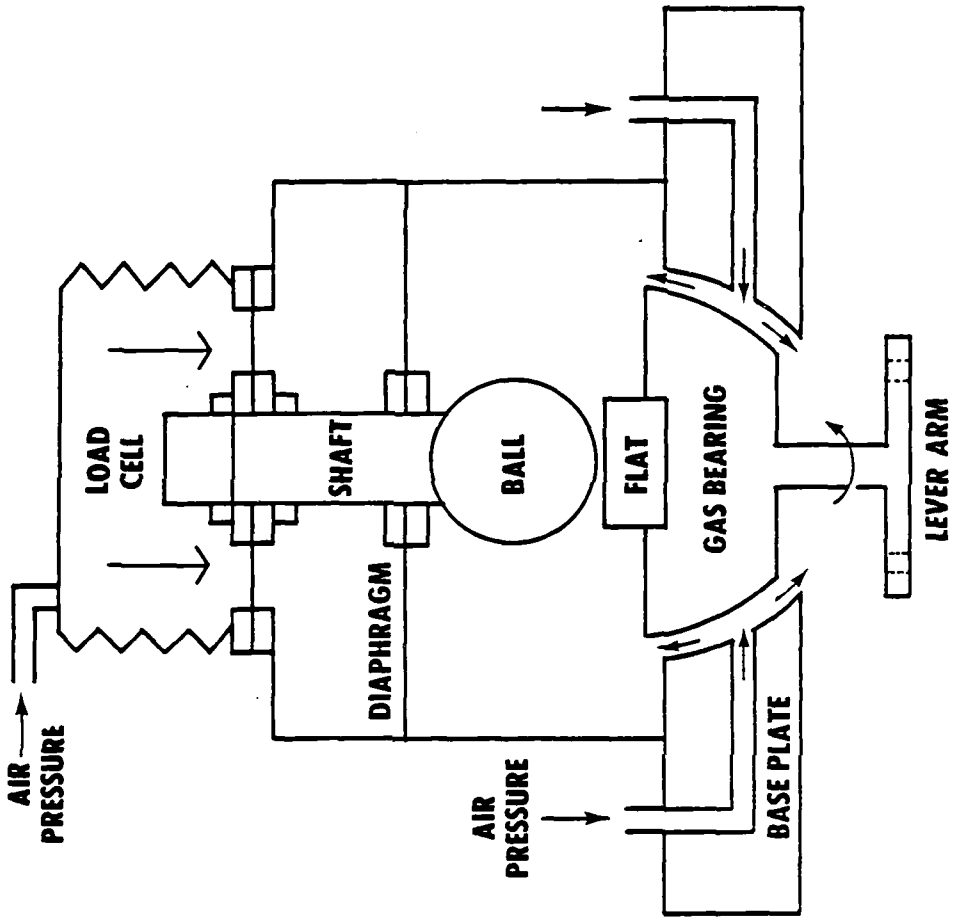

FIGURE 2. SCHEMATIC OF FRETTING TEST RIG

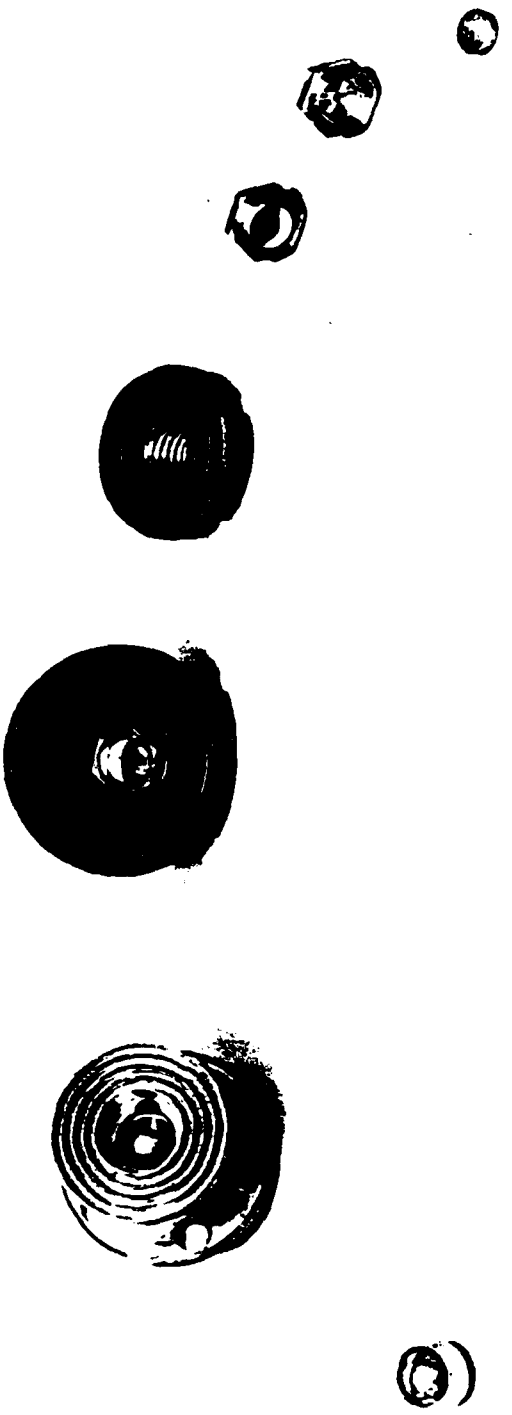

FIGURE 3. SPECIMENS AND LABYRINTH SEALS USED IN THE FRETTING TEST RIG

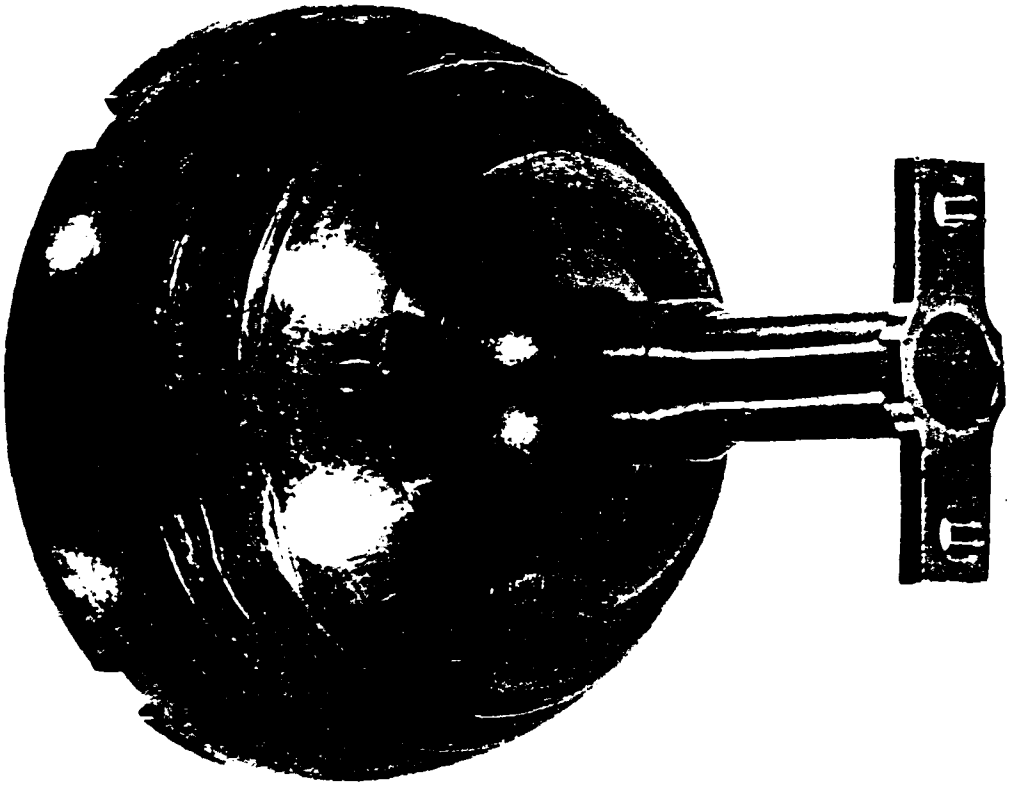

FIGURE 4. PHOTOGRAPH OF GAS BEARING

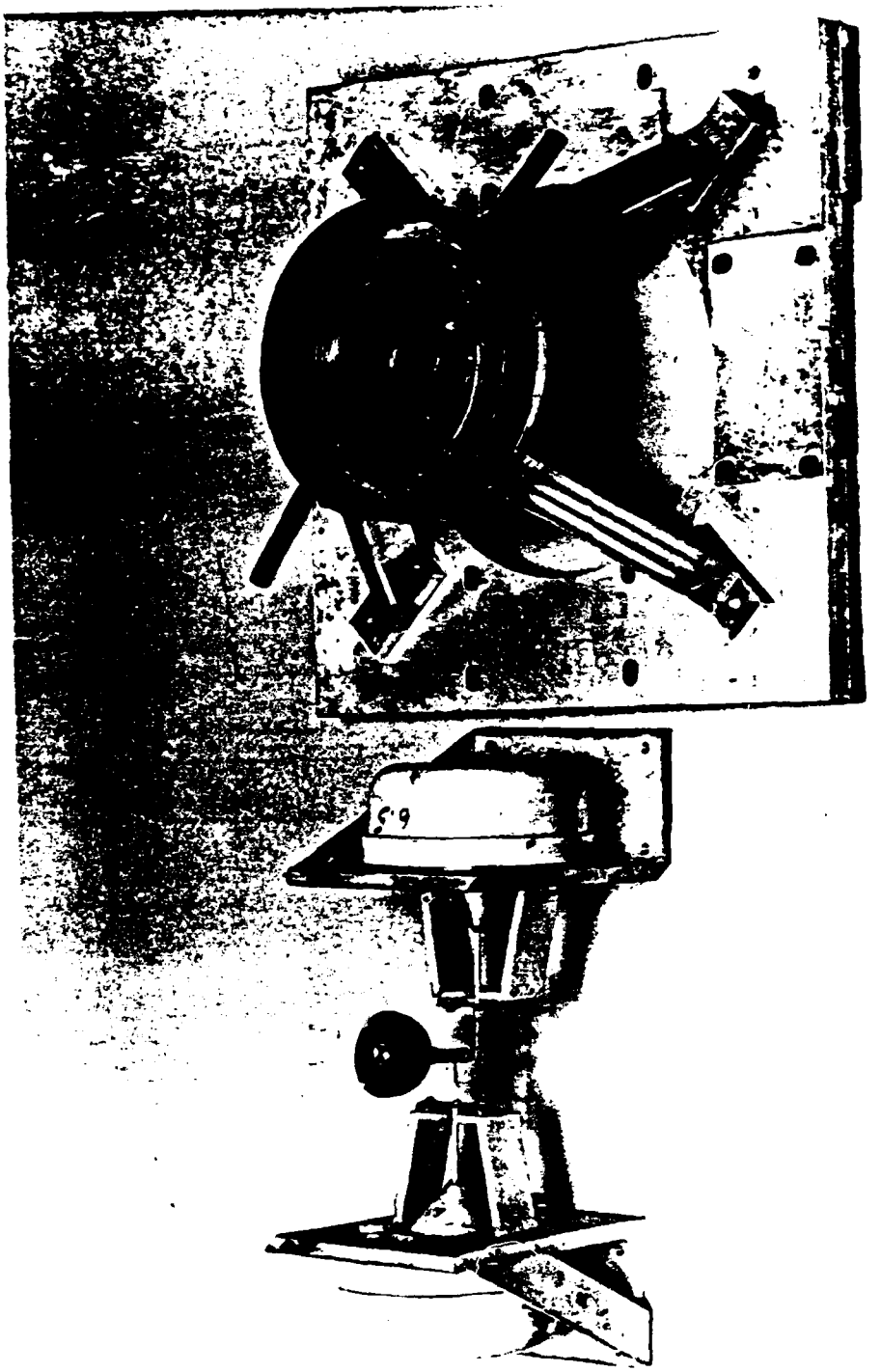

FIGURE 5. BASE PLATE OF FRETTING TEST RIG AND ATTACHMENT OF THE GAS BEARING TO THE DRIVE UNIT

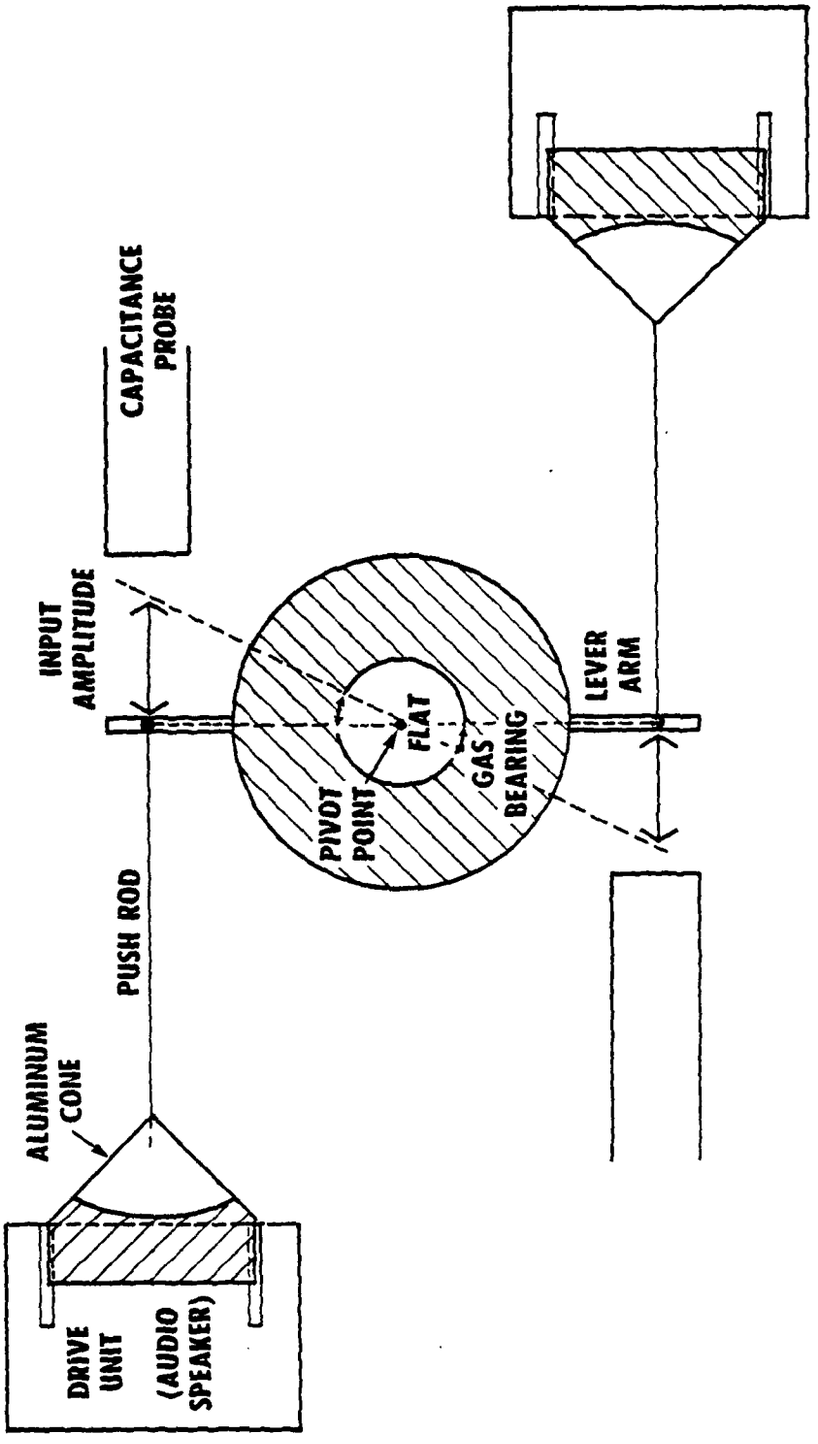

FIGURE 6. ELECTROMAGNETIC DRIVE UNIT AND SPECIMEN MOTION

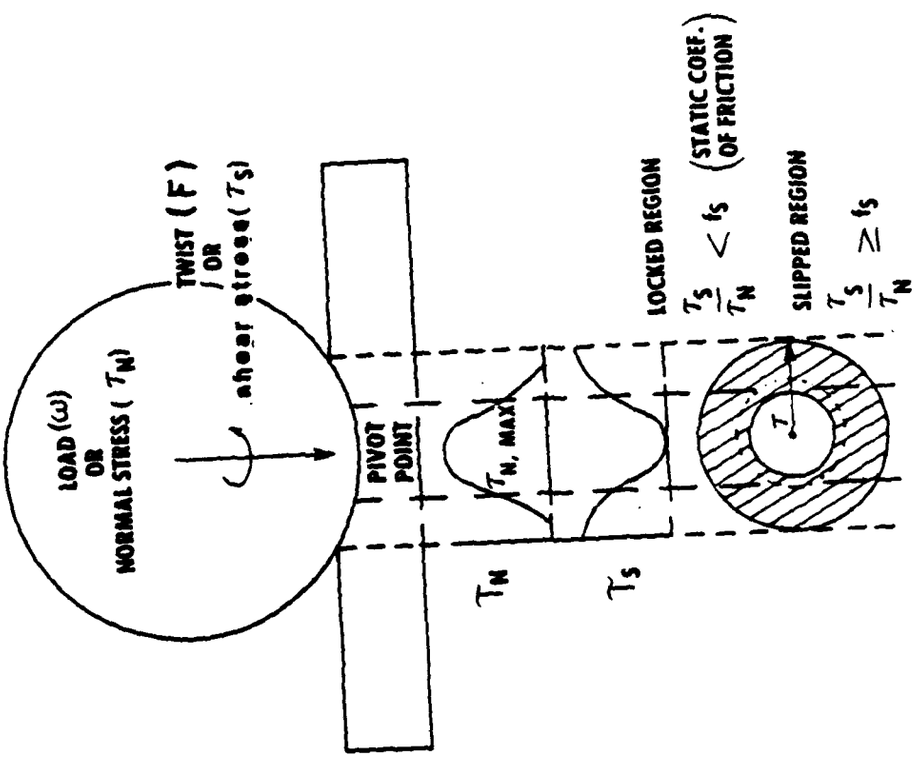

FIGURE 7. BALL ON FLAT CONFIGURATION

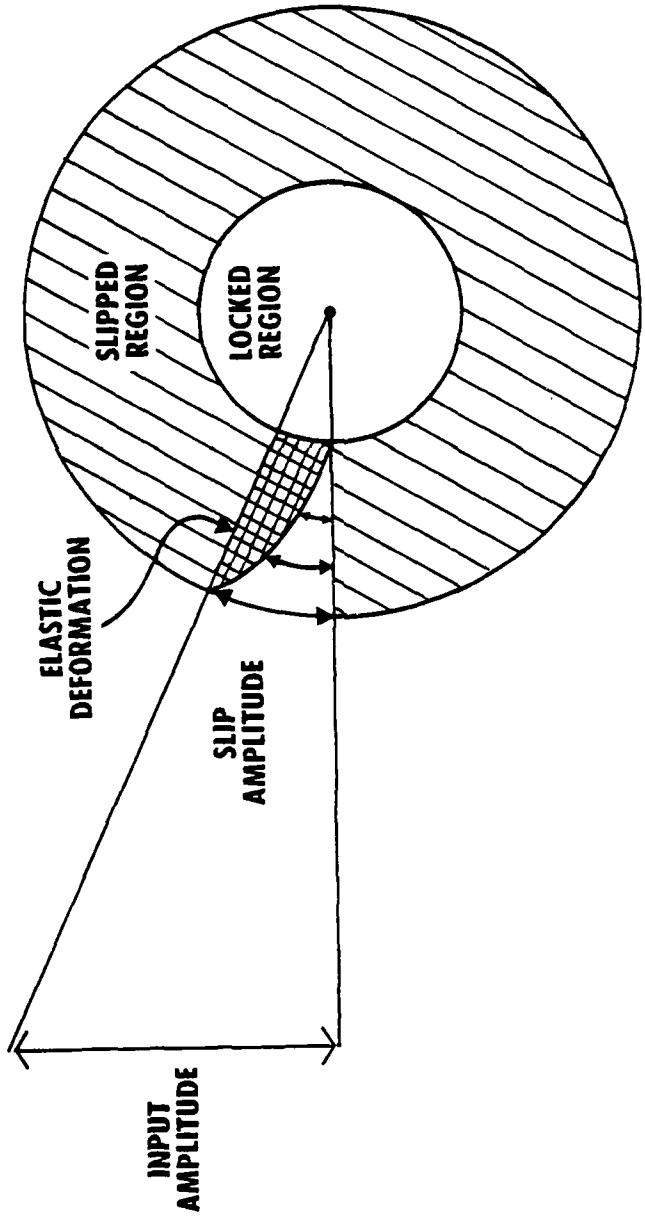

FIGURE 8. RELATIONSHIP OF MICROSLIP TO DISPLACEMENT

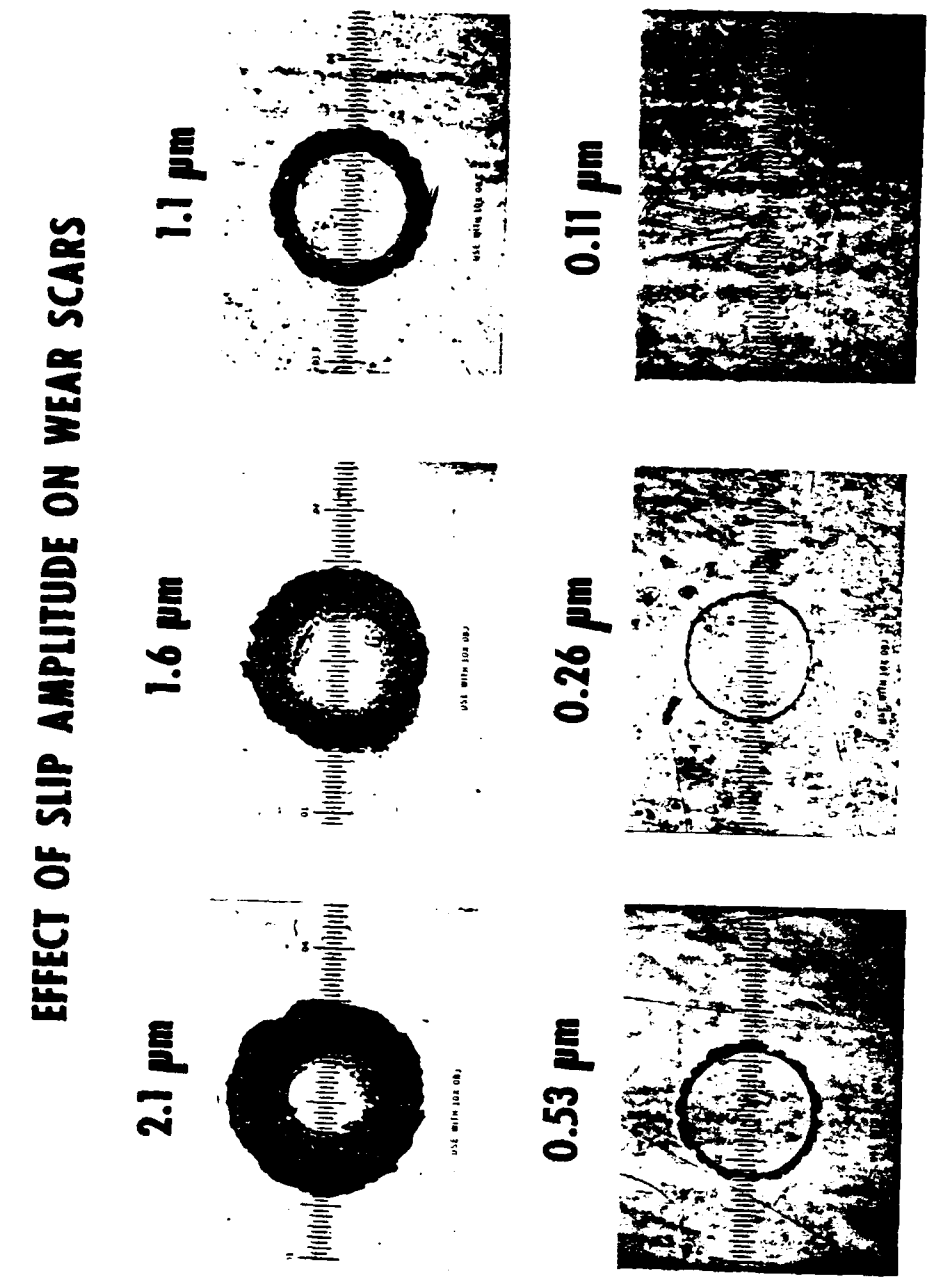

FIGURE 9. WEAR SCARS AT 100X MAGNIFICATION

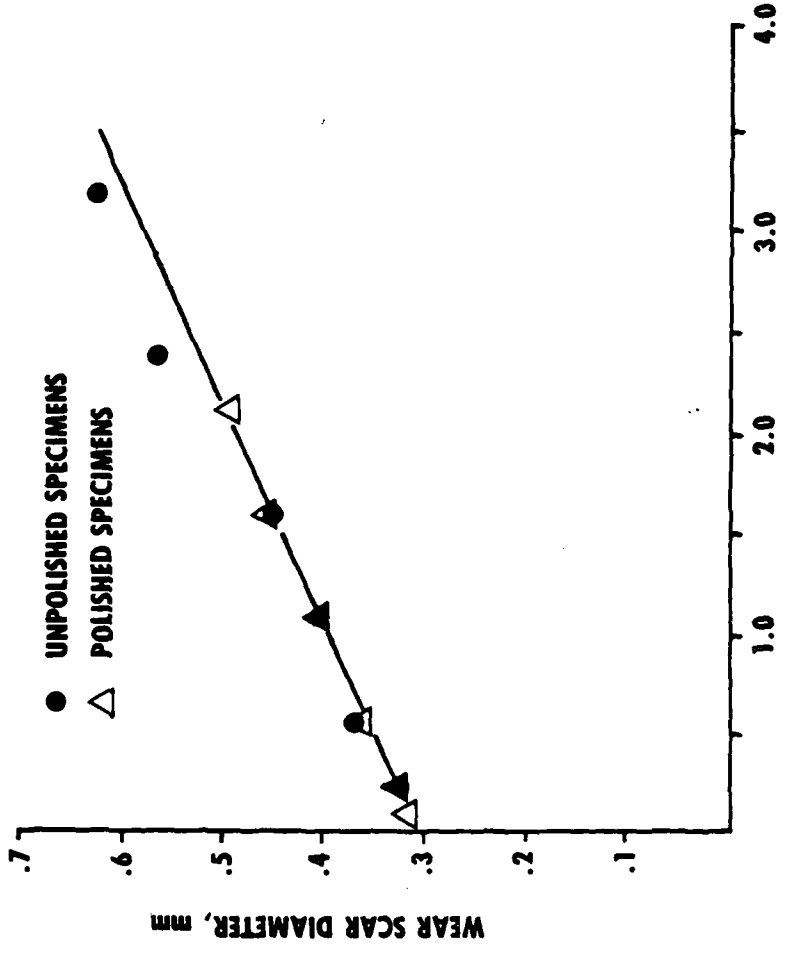

FIGURE 10. EFFECT OF SLIP AMPLITUDE ON THE DIAMETER OF THE WEAR SCAR

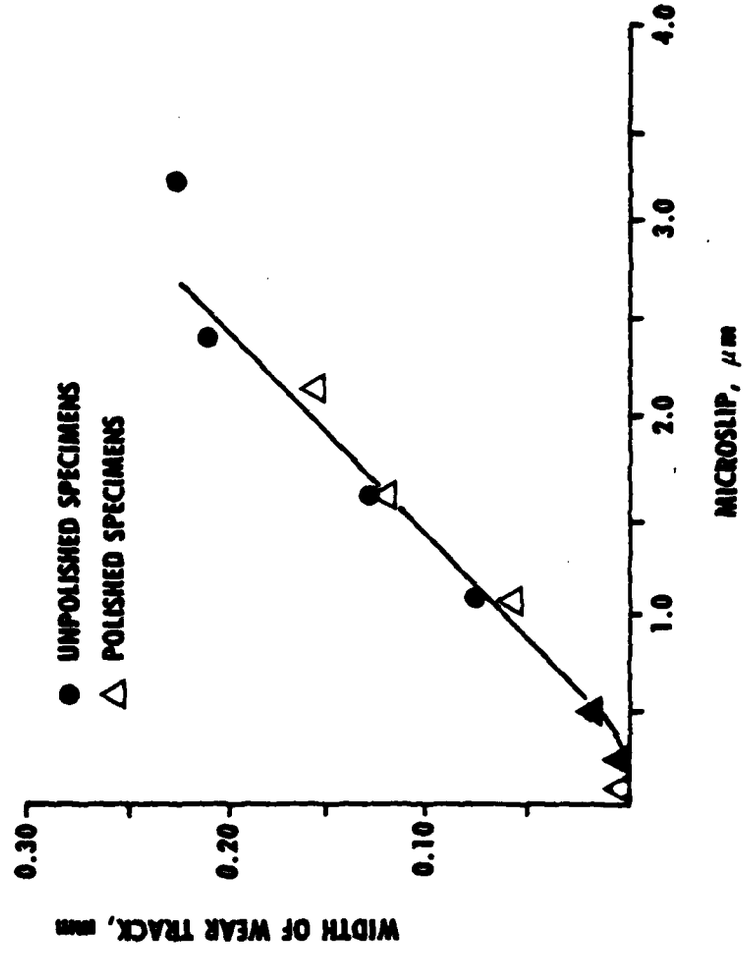

FIGURE 11. EFFECT OF SLIP AMPLITUDE ON THE WIDTH OF THE SLIPPED REGION

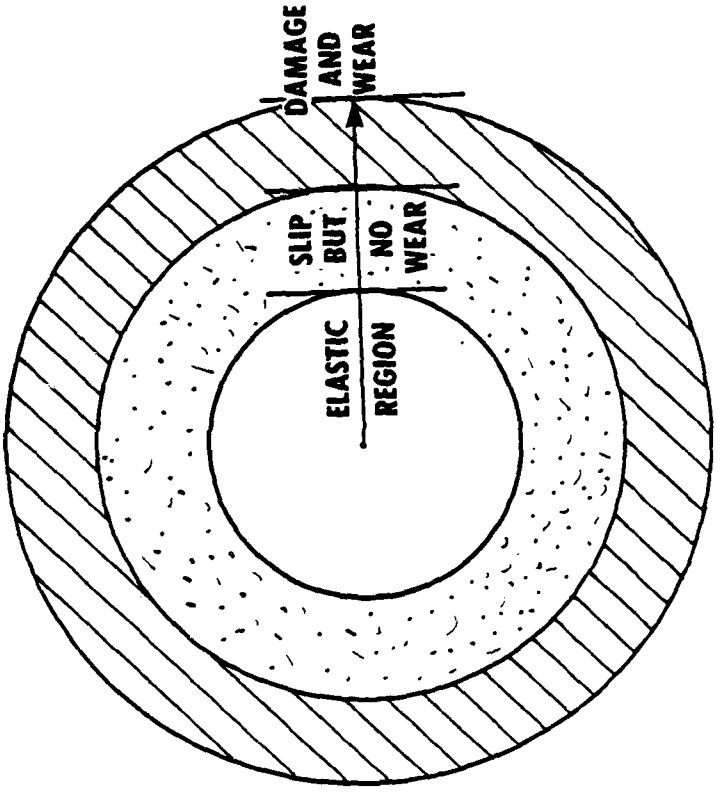

FIGURE 12. WEAR SCAR MODEL THAT ALLOWS FOR SLIP WITHOUT DAMAGE

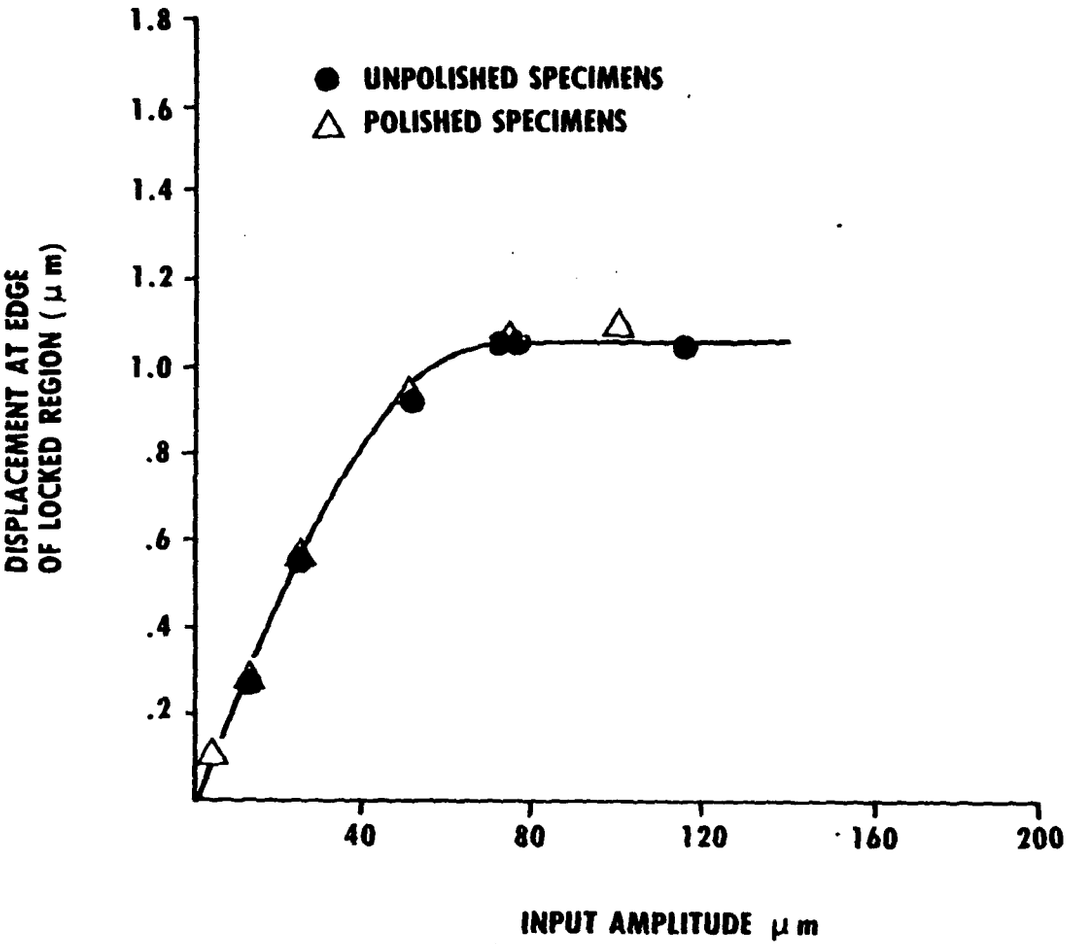

FIGURE 13. THE EFFECT OF INPUT AMPLITUDE ON DISPLACEMENT AT THE EDGE OF THE LOCKED REGION

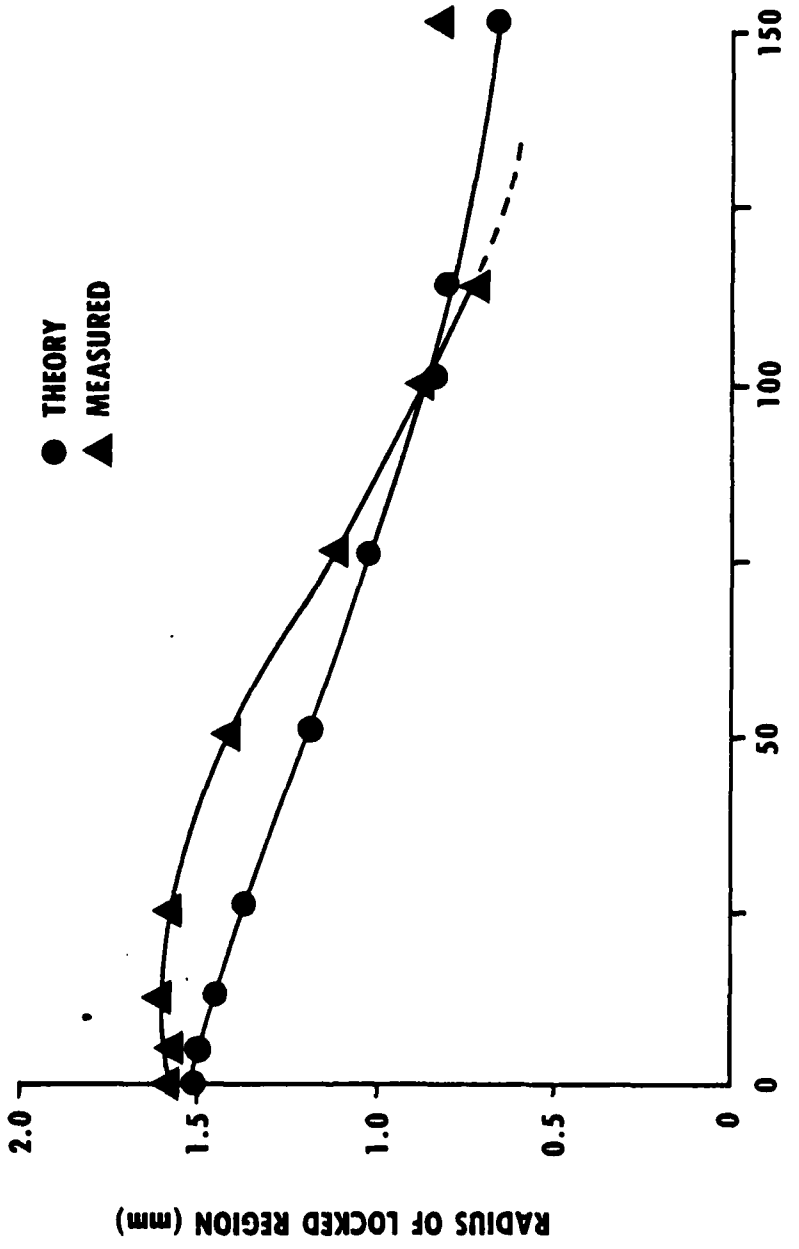

FIGURE 14. A COMPARISON OF THE THEORETICAL RADIUS OF THE LOCKED REGION WITH EXPERIMENTAL DATA

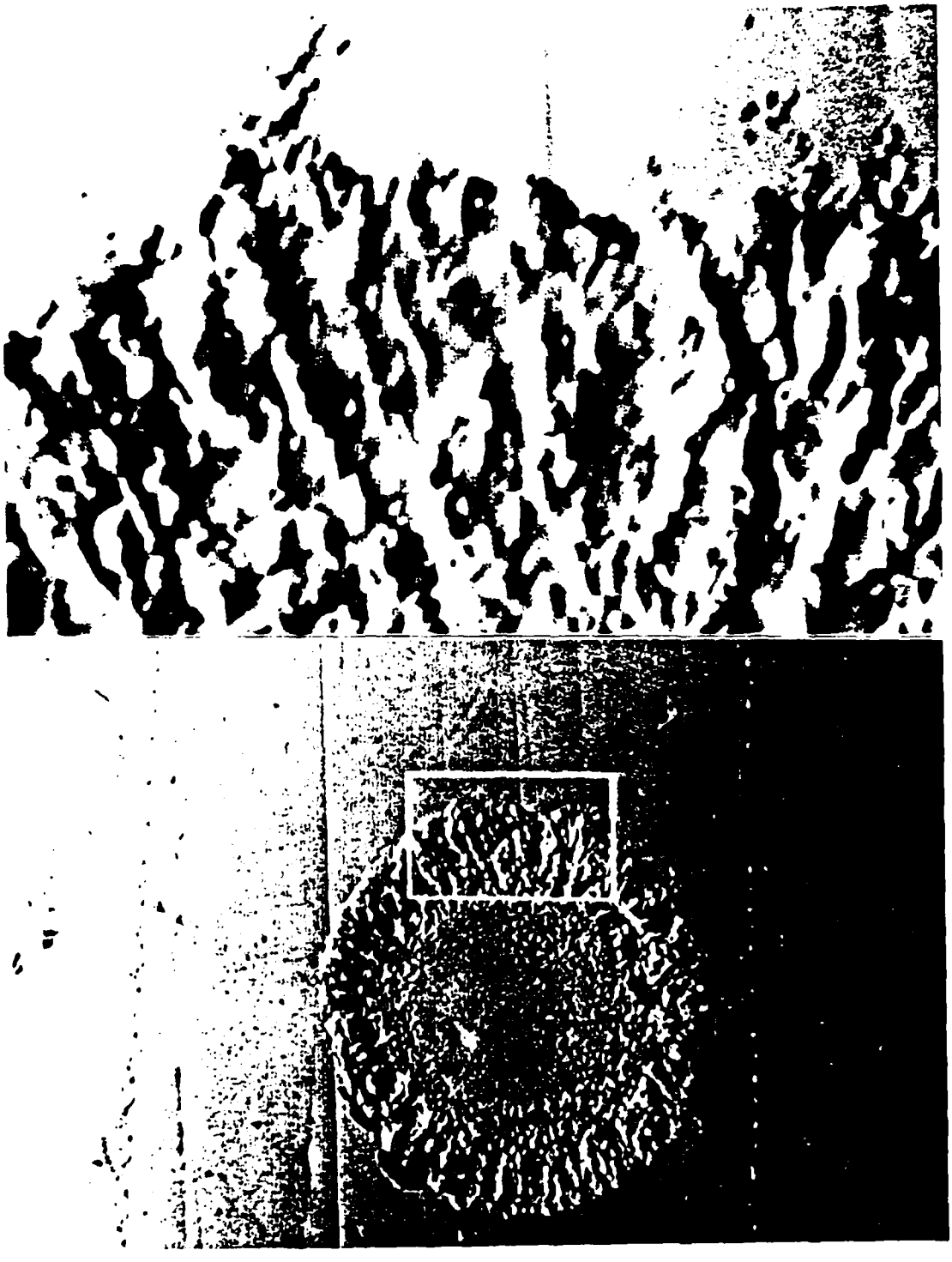

FIGURE 15. PHOTOMICROGRAPH OF WEAR SCAR AT 65X MAGNIFICATION AND EXPANDED VIEW OF SLIPPED REGION AT 325X MAGNIFICATION

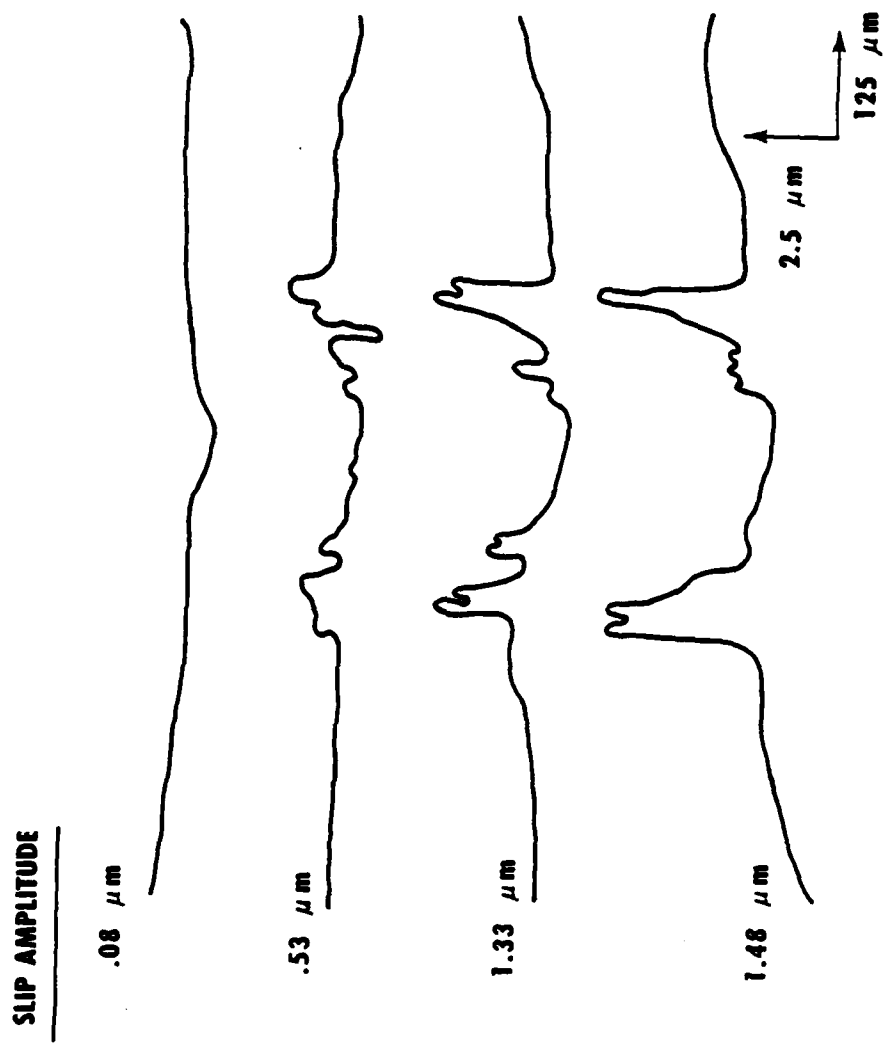

FIGURE 16. THE EFFECT OF SLIP AMPLITUDE ON THE SURFACE PROFILE OF WEAR SCARS

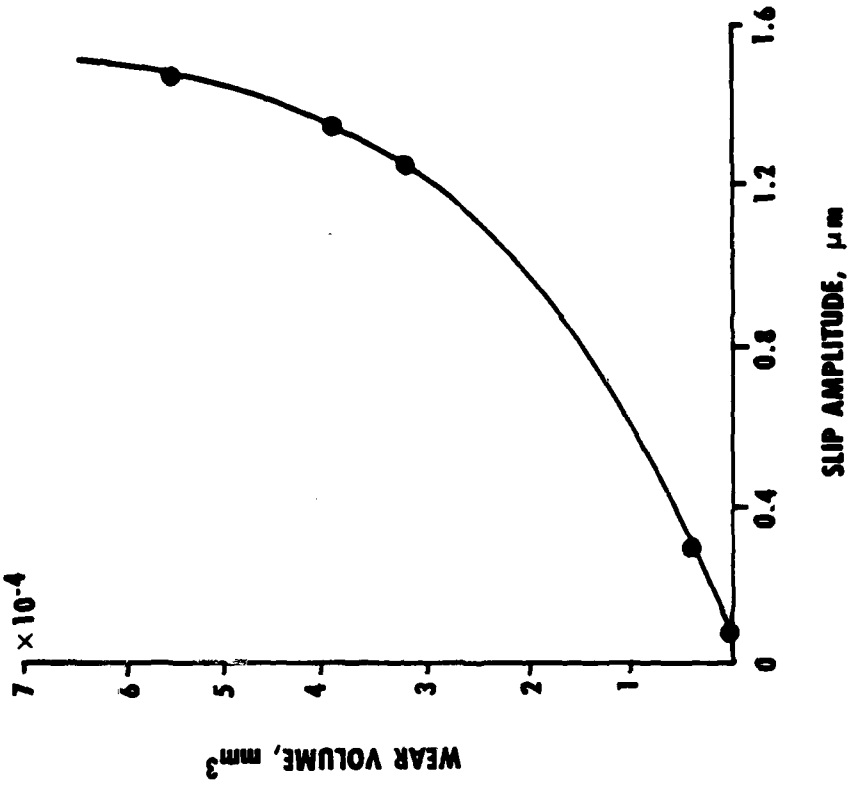

FIGURE 17. WEAR VOLUME AS A FUNCTION OF SLIP AMPLITUDE


DATE
ILME